Plant Physiology and Biochemistry 136 (2019) 215–221

Contents lists available at ScienceDirect

Plant Physiology and Biochemistry

journal homepage: www.elsevier.com/locate/plaphy

Research article

SbRFP1 regulates cold-induced sweetening of potato tubers by inactivation of StBAM1

Huiling Zhang[a,b], Ying Yao[a], Shuangchen Chen[b], Juan Hou[a,c], Yihe Yu[b], Tengfei Liu[a], Juan Du[a], Botao Song[a,*], Conghua Xie[a]

[a] Key Laboratory of Horticultural Plant Biology (HZAU), Ministry of Education, Key Laboratory of Potato Biology and Biotechnology, Ministry of Agriculture and Rural Affairs, Huazhong Agricultural University, Wuhan, 430070, People's Republic of China
[b] College of Forestry, Henan University of Science and Technology, Luoyang, 471000, People's Republic of China
[c] College of Horticulture, Henan Agricultural University, Zhengzhou, 450002, People's Republic of China

ARTICLE INFO

Keywords:
Potato
Cold-induced sweetening
SbRFP1
Ubiquitination degradation
StBAM1

ABSTRACT

Potato cold-induced sweetening (CIS) is a major drawback restricting potato process industry. Starch degradation and sucrose decomposition are considered to be the key pathways in potato CIS. Our previous study showed that the RING finger gene *SbRFP1* could slow down starch degradation and the accumulation of reducing sugars (RS) through inhibiting amylase and invertase activity in cold-stored tubers. However, the regulation mechanism of *SbRFP1* is not clear. In this paper, we first proved that SbRFP1 could promote starch synthesis and modify the shape of starch granules. By further yeast two hybrid, GST-pull down and inhibition of enzyme activity assays, we confirmed that SbRFP1 could slow down the transformation of starch to RS in tubers mainly through the inhibition of β-amylase StBAM1 activity. SbRFP1 was also proved to possess E3 ubiquitin ligase activity by ubiquitination assay. Thus, SbRFP1 may regulate the accumulation of RS in cold-stored tubers by ubiquitination and degradation of StBAM1. Therefore, our study reveals the regulatory mechanism of SbRFP1 in the process of CIS and provides more powerful evidence for the effect of starch degradation on potato CIS.

1. Introduction

Potato (*Solanum tuberosum* L.) is the most important non-grain food crop in the world. For a continuous supply of raw material, potato tubers are often stored at low temperature to reduce sprouting, water loss and pathogenesis. However, low temperature induces the accumulation of reducing sugar (RS), which is known as cold-induced sweetening (CIS). RS can react with the α-amino acid groups of nitrogenous compounds from nonenzymatic Maillard reactions during frying, resulting in dark-colored food products and, more worrying, generating the carcinogen acrylamide (Shepherd et al., 2010). Therefore, CIS poses a significant challenge to the potato industry and raise a worldwide food safety concern (Xin and Browse, 2000; Mottram et al., 2002; Halford et al., 2012).

Starch degradation and sucrose hydrolysis have been reported to be the main pathways involved in potato CIS (Bhaskar et al., 2010; Zhang et al., 2014a; Lin et al., 2015; Hou et al., 2017). The starch degradation pathway mainly involves enzymes such as α-amylase (EC 3.2.1.1), β-amylase (EC 3.2.1.2), and the starch phosphorylase (EC 2.4.1.1) (Preiss, 1982; Solomos and Mattoo, 2005). In cold-stored potato tubers, β-amylase may play important roles in RS accumulation. It was reported that when the storage temperature was reduced from 20 °C to 5 °C or 3 °C, the β-amylase activity in potato tubers increased four to five fold over a 10-day period (Nielsen et al., 1997). Several β-amylase genes in the potato genome database have been identified, and the association of their gene expression patterns with RS content and amylase activities has been investigated. Results showed that the β-amylase activity primarily reflected by StBAM1 and StBAM9 and thus indicated that the β-amylase might play an important role in RS accumulation in tubers stored at low temperatures (Zhang et al., 2014a). Further functional studies of amylase genes reveals they function in different ways. StBAM1 regulated CIS by hydrolyzing soluble starch, StBAM9 by directly acting on starch granules, while StAmy23 by degrading cytosolic phytoglycogen (Hou et al., 2017). However, the regulation mechanism of amylase genes still needs further exploration.

Previously, we proved that a RING finger gene *SbRFP1* played a negative role in amylase activity and starch degradation of potato CIS (Zhang et al., 2013). However, the regulation mechanism of *SbRFP1* on

* Corresponding author. Key Laboratory of Horticultural Plant Biology (HZAU), Ministry of Education, Key Laboratory of Potato Biology and Biotechnology, Ministry of Agriculture and Rural Affairs, Huazhong Agricultural University, Wuhan, 430070, People's Republic of China.
E-mail address: lug109@163.com (B. Song).

https://doi.org/10.1016/j.plaphy.2019.01.019
Received 18 October 2018; Received in revised form 7 January 2019; Accepted 14 January 2019
Available online 19 January 2019
0981-9428/

amylase and invertase is not clear. RING finger proteins constitute a large protein family in higher plants and are involved in various signal transduction pathways (Chen and Ni, 2006; Jung et al., 2013). Such proteins can affect the physiological processes of plants by regulating gene expression. Arabidopsis overexpressing RING-H2 gene, *XERICO*, exhibited hypersensitivity to salt and osmotic stress as well as exogenous abscisic acid (ABA) during germination and early seedling growth. And Affymetrix GeneChip array analysis showed that the expressions of many of the genes involved in the biosynthesis of plant hormones were significantly changed in the overexpression transgenic plants (Ko et al., 2006). A C3HC4 RING finger gene from rice, *OsDIS1*, is involved in drought-stress signal transduction. Overexpression of *OsDIS1* reduced drought tolerance in transgenic rice plants, while RNAi silencing of *OsDIS1* enhanced drought tolerance. Microarray analysis revealed that a large number of drought-responsive genes were induced or suppressed in the *OsDIS1* overexpression plants under normal and drought conditions (Ning et al., 2011), the results showed that *OsDIS1* played a negative role in regulating drought resistance through regulating the expression of stress related genes.

The RING finger domain also functions as protein-protein interaction site and has been reported to play important roles as ubiquitin ligases E3 in post-translational regulation (Lee and Kim, 2011; Ning et al., 2011). *Arabidopsis thaliana* RING finger protein AIP2 could interact and polyubiquitinate ABI3, which is a central regulator in ABA signaling. And AIP2-overexpression plants contained lower levels of ABI3 protein than wild type and were more resistant to ABA, this showed that AIP2 negatively regulates ABA signaling by targeting ABI3 for post-translational destruction (Zhang et al., 2005). Arabidopsis RING finger protein HOS1 is an E3 ligase. HOS1 physically interacts with ICE1, a transcription factor which can activate the expression of CBFs, and mediates the ubiquitination of ICE1 both *in vitro* and *in vivo*. So overexpression of *HOS1* could repress the expression of CBFs and their downstream genes and conferred increased sensitivity to freezing stress in plant (Dong et al., 2006).

In this study, we further characterized the effects of SbRFP1 on CIS of potato tubers and explore its regulation mechanism.

2. Materials and methods

2.1. Plant materials and treatments

The over-expressing (OE) and RNAi (RI) transgenic lines of *SbRFP1* and untransformed controls from a previous study (Zhang et al., 2013) were used. And they were grown in 24-cm-diameter plastic pots in the greenhouse at National Centre for Vegetable Improvement (Central China) (Wuhan, China) at 20–25 °C and with 12 h of light per day under mercury lamp. After two months, the mature leaves were sampled at the following time points: 0 h, 6 h, 12 h, 18 h and 24 h, respectively. The sampled leaves were immediately frozen in liquid nitrogen and stored at −70 °C until use. When the leaves senesced naturally, the mature tubers were harvested. *Nicotiana benthamiana* plants were grown at 20–25 °C in 10-cm-diameter plastic pots in the greenhouse at Huazhong Agricultural University (Wuhan, China) with 16 h of light per day as supplemented with mercury lamps.

2.2. Assessing the starch content and starch granule

The starch content was determined as previously detailed (Liu et al., 2010). The starch granule of potato tubers was measured according to Li et al. (2011). Potato pieces were squeezed with a garlic press, and then 3 μL juice was directly transferred to a round chamber containing 7 μL water and mixed well with the pipette tip immediately. From separate areas each with approximately 200 starch granules, images were randomly recorded by a Carl Zeiss light microscope with a 20× microscopic objective and a polarizer, and processed by AxioVision Rel 4.7 software (Carl Zeiss, Germany). Three images were used to measure the length and width of starch granules. The statistical analysis was done with SAS 8.1 (SAS Institute Inc, USA).

Table 1
The primer sequences for constructing vectors.

Primer name	Primer sequences (5' – 3')
SbRFP1 pro L	CGGGATCCATGGCTCGCGTAATCTGATATC
SbRFP1 pro R	CATGCGGCCGCTTAACGAGTCTGGCAATTCCAATG
sbrfp1proL	GGTGTATACATCGCTTGCAGGTGTAAAGAGGAATT
sbrfp1proR	CCACATCCGTAGCTAAATTCCTCTTTACACCTGCA
SbRFP1DL	AAAAAGCAGGCTCAATGGCTCCGCGTAATCTGATATC
SbRFP1DR	AGAAAGCTGGGTATTAACGAGTCTGGCAATTCCAATG
BK-SbRFP-F	ATGGCCATGGAGGCCGAATTCATGGCTCCGCGTAATCTGAT
BK-SbRFP-R	ATGCGGCCGCTGCAGGTCGACTTAACGAGTCTGGCAATTCC
BK-SbRFP(1-102)-F	GGCCATGGAGGCCGAATTCATGGCTCCGCGTAATCTGAT
BK-SbRFP(1-102)-R	GCGGCCGCTGCAGGTCGACTTATTCCCTTTGAAACTGTTGAC
BK-SbRFP (103-167)-F	GGCCATGGAGGCCGAATTCATGCAACAGTTTCAAAGGGAAGAA
BK-SbRFP (103-167)-F	GCGGCCGCTGCAGGTCGACTTAACGAGTCTGGCAATTCCA

2.3. Subcellular localization of SbRFP1

The cDNA of *SbRFP1* was amplified with primers SbRFP1DL and SbRFP1DR (Table 1) and then subcloned into a pK7FWG2 vector for the purpose of fluorescent tagging of SbRFP1 by recombination (Helliwell et al., 2002). The recombinant plasmid named pK7FWG2-SbRFP1 was confirmed by sequencing (BGI, Wuhan, China) and then introduced into *Agrobacterium tumefaciens* strain GV3101.

Fully developed leaves of 3–4 week-old *Nicotiana benthamiana* were used for agroinfiltration. Approximately 300 μL of *Agrobacterium* culture containing pK7FWG2-SbRFP1 was infiltrated at four points. At two days post infiltration, fluorescence detection was performed using a confocal laser scanning microscope (LSM510 Meta, Zeiss, Germany). Fluorescence signals were detected and recorded by LSM Image Examiner software (Zeiss, Germany).

2.4. Yeast two-hybrid assays

A prey library was generated using the cDNA of CIS-resistant *Solanum berthaultii* (accession CW2-1) tubers stored at 4 °C for 5 days, and then transferred into the yeast stain Y187 using BD Matchmaker™ Library Construction Kit following the yeast two-hybrid (Y2H) protocols provided therein (Clontech, Germany). The quality of the library was also tested following the protocols.

The 1-102 amino acid of *SbRFP1* was inserted into the *Eco*RI/*Bam*HI restriction sites of pGBKT7 vector (named pGBKT7-SbRFP1102) before transforming into yeast stain AH109 as described in the protocols of the BD MatchmakerTM Screening Kit. Subsequently, the X-α-Gal assay was subjected by following the instruction of the Yeast Protocols Handbook. The positive clones were sequenced (BGI, Wuhan, China). Primers are listed in Table 1.

2.5. Protein expression and interaction proteins analysis

The cDNA of *SbRFP1* was amplified with primers SbRFP1proL and SbRFP1proR (Table 1) and then subcloned into a pGEX-6p-1 vector. The 5′ end of mutant sequences sbrfp1 were obtained with the primers SbRFP1proL and sbrfp1proR (Table 1) (in which "TGC" were replaced by "AGC", encoding 150th amino acid in SbRFP1), and the 3′ end were obtained with the primers sbrfp1proL (in which "CAC" were replaced by "UAC", encoding 140th amino acid in SbRFP1) and SbRFP1proR (Table 1). Then sbrfp1 sequences (the 140th histidine of *SbRFP1*

replaced by tyrosine and the 150th cysteine replaced by serine) were obtained by reconstructing the 5′ end and 3' end with the primers SbRFP1proL and SbRFP1proR. After sequenced, the sbrfp1 sequences were subcloned into the expression vector pGEX-6p-1, named pGEX-sbrfp1. The pGEX-SbRFP1 and pGEX-sbrfp1 plasmids which contained GST tag from pGEX-6p-1 were transformed into *E. coli* BL21 (DE3). The plasmids were expressed at 37 °C under induction with 0.02 mM IPTG for 4 h. The protein purification was performed by following the Gravity Purification protocol as described previously (Tai et al., 2010). With the same methods, the StBAM1 sequences were subcloned into the expression vector pET28a, named pET-StBAM1. Then pET-StBAM1 was transformed into *E. coli* BL21 and expressed at 37 °C under induction with 0.01 mM IPTG for 2 h. StAmy23 and StvacINV1 were subcloned into the pPIC9k vector and transformed into yeast GS115 strain, and the protein was purified according to the manual (Invitrogen, Carlsbad, CA) (Zhang et al., 2014b).

Interaction protein analysis was performed by the method of GST Pull-down (Tai et al., 2010; Han et al., 2015). SbRFP1 protein which is GST-tagged was mixed with StBAM1 and StAmy23 respectively (the concentration ratio was 1:3). And 200 μL activated glutathione resin was added into the system, and the volume was supplemented by 5 ml in a buffer. After incubated in a shaker at 4 °C for 2 h, the solution was transferred into a column and left at 4 °C for 30 min. Then wash and collect proteins according to the Gravity Purification protocol.

2.6. The amylase activity analyses

The inhibitory tests of SbRFP1and sbrfp1 to amylase activity were performed with kits from Megazyme (Bray, Ireland). pGEX-SbRFP1 or pGEX-sbrfp1 and the enzymes were pre-incubated for 30 min at 40 °C, and then 20 μL (5 U/mL) p-nitrophenyl-α-D-maltoheptaoside (the substrate for α-amylase) or p-nitrophenyl-β-D-maltoheptaoside (the substrate for β-amylase) was added and incubated for 15 min at 40 °C. The reaction was stopped by adding 2% Tris base to the stop solution, and the absorbance was measured at 405 nm with pGEX-6P-1 as control.

2.7. E3 ubiquitin ligase activity assay

The ubiquitination assays *in vitro* were performed using the Auto-ubiquitinylation kit (Enzo Life Sciences) following the instruction Manual BML-UW0970. Each reaction (50 μL final volume) contained 2.5 μL 20 × E1, 2.5 μL 20 × E2, 5 μL 10 × Ub E3 ligase buffer, 5 μL 10 × ubiquitin, 1 μL 50 mM DTT, 2.5 μL Mg-ATP, and 2.5 μL of pGEX-SbRFP1 protein or pGEX-sbrfp1 protein or 20 × E3 control. The mixture was incubated at 37 °C for 1 h. Quench assays were performed by addition of 50 μL 2 × SDS PAGE gel loading buffer, heated to 95 °C for 5 min, and analyzed by SDS-PAGE electrophoresis. Following blotting, hybridization was performed using ubiquitin antibody and Goat Anti-Rabbit lgG-peroxidase antibody (Sigma, A0545).

3. Results

3.1. SbRFP1 could promote starch synthesis and modify the shape of starch granules

In our previous research, the change of starch content in transgenic tubers before and after storage at low temperature showed that the starch degradation rate was significantly inhibited in the tubers from transgenic lines over-expressing (OE) *SbRFP1* gene and elevated in the RNAi (RI) transgenic tubers (Zhang et al., 2013). In order to further clarify the effect of *SbRFP1* on starch, OE- and RI-transgenic plants were studied. The starch content in leaves at different illumination time and the shape of starch granules in tubers were measured. Results show that the starch content of OE-transgenic lines is significantly higher than that of the control E3 at the time points 6 h and 12 h, while the starch content of RI-transgenic lines (except RI-13) is significantly lower than that of the control AC142 at the time points 6 h, 12 h and 18h (Fig. 1). Compared with their controls, the length width ratio of starch granules was significantly increased in OE-transgenic tubers and decreased in RI-transgenic tubers, respectively (Fig. 2). All the results proved that *SbRFP1* could promote starch synthesis and modify the shape of starch granules.

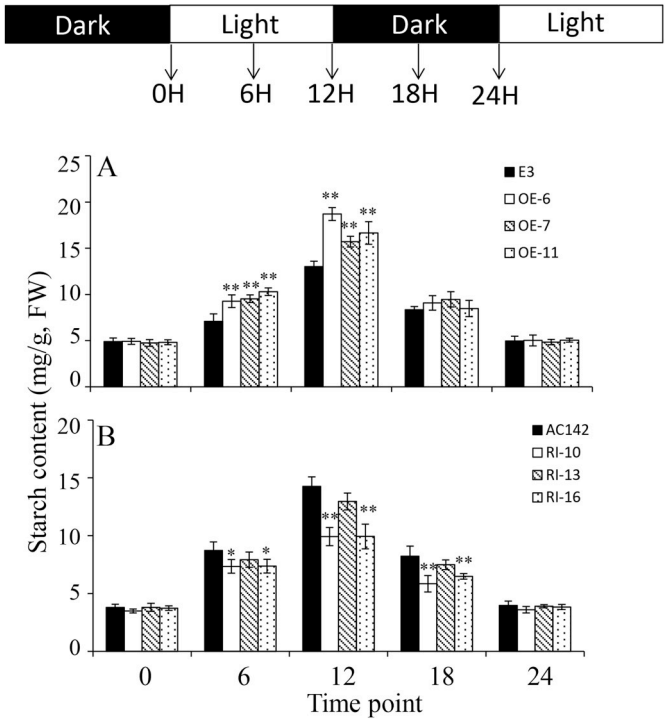

Fig. 1. The starch contents of the leaves at different time points. A: The starch contents in leaves of OE-transgenic lines and the control E3. B: The starch contents in leaves of RI-transgenic lines and the control AC142. Columns represent mean values ± SE (n = 3) (*P < 0.05; **P < 0.01).

3.2. SbRFP1 is mainly located in the nucleus and cytoplasm

To study the sublocalization of SbRFP1, we constructed a recombinant vector pK7FWG2-SbRFP1, in which SbRFP1 was fused to an enhanced green fluorescent protein (eGFP). pK7FWG2-SbRFP1 was then transiently expressed in *Nicotiana benthamiana* leaves by agroinfiltration. The green fluorescence was mainly found in the nucleus and cytoplasm (Fig. 3), suggesting that SbRFP1 is mainly located in the nucleus and cytoplasm.

3.3. Screening and verification of the interaction proteins of SbRFP1

To further characterize the role of SbRFP1 in the process of potato CIS, yeast two hybrid method was used to identify its interacted proteins. Because the full-length cDNA and the 103-167 amino acid of SbRFP1 were shown to have auto-activation, pGBKT7-SbRFP1102 vector (including the 1-102 amino acid of SbRFP1) was constructed as bait for screening Y2H library above. To select positive clones, the diploids were further assayed by X-α-Gal (5-Bromo-4-chloro-3-indoxyl-α-D-galactopyranoside) to preclude positive false results. The survival and blue color of the clones (positive clones) on SD/-Leu-Trp-His-Ade/X-α-Gal selecting plates represent the putative interaction. About 100 positive clones were obtained and sequenced. By BLAST to PGSC database (http://solanaceae.plantbiology.msu.edu/integrated_searches.shtml), we selected 36 potential SbRFP1-interacted proteins, which are mainly related to starch metabolism and transcription factors including

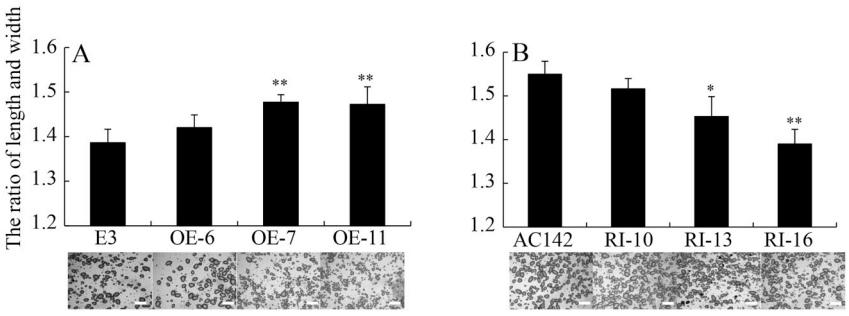

Fig. 2. The length to width ratio and pictures of transgenic tubers starch granules. A: The length to width ratio and pictures of OE-transgenic tubers starch granules and the control E3. B: The length to width ratio and pictures of RI-transgenic tubers starch granules and the control AC142. Columns represent mean values ± SE (n = 3) (*P < 0.05; **P < 0.01). Bar: 100 μm.

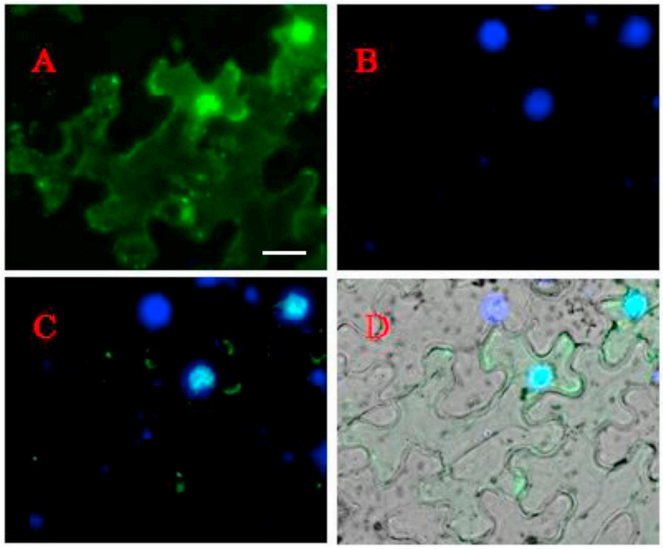

Fig. 3. Subcellular localization of SbRFP1 in *Nicotiana benthamiana* leaves. A: image of the GFP fluorescence of transient expression pK7FWG2-SbRFP1shows GFP signals mainly in nucleus and cytoplasm. Bar: 10 μm. B: image of a nucleus stained with DAPI. C and D: merged images.

StBAM1 and StAmy23 (Table 2). Since our previous studies indicated that SbRFP1 might have an effect on amylase and invertase (Zhang et al., 2013), we further tested interaction by GST-pull down method. pGEX-SbRFP1 (Fig. 4A) and PET-StBAM1 were purified from *E.coli*, and StAmy23 was purified from yeast (Zhang et al., 2014b). pGEX-SbRFP1 was incubated with StAmy23 and PET-StBAM1 individually. Except for pGEX-SbRFP1, the eluted protein from cartridge contains StAmy23 (Fig. 4C) or PET-StBAM1 (Fig. 4D). Results proved that SbRFP1 interacted with StBAM1 and StAmy23, respectively.

The invertase genes were not found in the positive clones, but previous studies showed that invertase activity in transgenic tubers would change (Zhang et al., 2013). So the invertase StvacINV1 was purified from yeast, and the interaction between SbRFP1 and StvacINV1 was tested by GST-pull down method also. After incubation of SbRFP1 and StvacINV1, the protein eluted from cartridge contains only SbRFP1 and no StvacINV1 (Fig. 4B), indicating that there is no interaction between SbRFP1 and StvacINV1.

3.4. His140 and Cys150 are important for the inhibition activity of SbRFP1 on StBAM1

In transgenic tubers, the activity of amylase was changed with the expression level of *SbRFP1* (Zhang et al., 2013). In order to further clarify whether SbRFP1 has direct effect on amylase activity of potato tubers, the crude protein of cold-stored potato tubers was extracted to determine the inhibitory effects of SbRFP1 on amylases. The results

Table 2
List of putative interaction proteins identified from the Y2H library.

number	Accession	Description
2_T7	XM_006367680	Solanum tuberosum NAC transcription factor 29-like
5_T7	XM_006340834	Solanum tuberosum beta-amylase 1(StBAM1)
8_T7	XM_001288450	Solanum tuberosum fructose-bisphosphate aldolase-like protein
9_T7	XM_006347569	Solanum tuberosum RNA pseudouridine synthase 7
10_T7	XM_015310649	Solanum tuberosum chaperone protein DnaJ-like
11_T7	XM_006343397	Solanum tuberosum probable E3 ubiquitin-protein ligase ARI9
13_T7	XM_006341127	Solanum tuberosum ribosomal protein L24-like protein
14_T7	XM_006350963	Solanum tuberosum actin-7-like
15_T7	XM_006360024	Solanum tuberosum polyubiquitin
17_T7	XM_006338668	Solanum tuberosum mitochondrial phosphate carrier protein 3
18_T7	XM_015303516	Solanum tuberosum transcription factor NF-Y CCAAT-binding-like
19_T7	XM_006340985	Solanum tuberosum 5-oxoprolinase
21_T7	S74514	Solanum tuberosum S-adenosylmethionine decarboxylase
22_T7	XM_006342848	Solanum tuberosum subtilisin-like protease SBT1.6
24_T7	XM_001287997	Solanum tuberosum flavonol synthase
26_T7	XM_004239815	Solanum lycopersicum putative F-box protein PP2-B12
27_T7	XM_006364505	Solanum tuberosum multiple organellar RNA editing factor 2
28_T7	XM_006364260	Solanum tuberosum transcription factor VOZ1-like
29_T7	XM_001287948	Solanum tuberosum low-temperature-induced cysteine proteinase-like
34_T7	XM_001288680	Solanum tuberosum S-adenosylmethionine synthase 1-like
38_T7	XM_006340597	Solanum tuberosum proteasome subunit beta type-1
43_T7	XM_015312555	Solanum tuberosum uncharacterized isomerase BH0283-like
44_T7	XM_006340105	Solanum tuberosum DNA-directed RNA polymerases II, IV and V subunit 11
45_T7	XM_006361772	Solanum tuberosum mitochondrial outer membrane protein porin
46_T7	XM_006338255	Solanum tuberosum protein furry homolog
48_T7	XM_006351253	Solanum tuberosum 37S ribosomal protein S9
52_T7	DQ235184	Solanum tuberosum clone 164A02 S-adenosyl methionine synthase-like
65_T7	M79328	Solanum tuberosum Alpha-amylase (StAmy23)
74_T7	XM_006338604	Solanum tuberosum glucose-6-phosphate 1-dehydrogenase
78_T7	XM_015314729	Solanum tuberosum protein SGT1 homolog A-like
81_T7	XM_006358693	Solanum tuberosum superoxide dismutase
83_T7	XM_006363267	Solanum tuberosum protein SRC2-like
84_T7	XM_006346747	Solanum tuberosum rho GDP-dissociation inhibitor 1-like
87_T7	XM_006349154	Solanum tuberosum putative methyltransferase C9orf114
88_T7	XM_006366505	Solanum tuberosum peptidyl-prolyl cis-trans isomerase Pin1-like
91_T7	NM_001287948	Solanum tuberosum low-temperature-induced cysteine proteinase-like

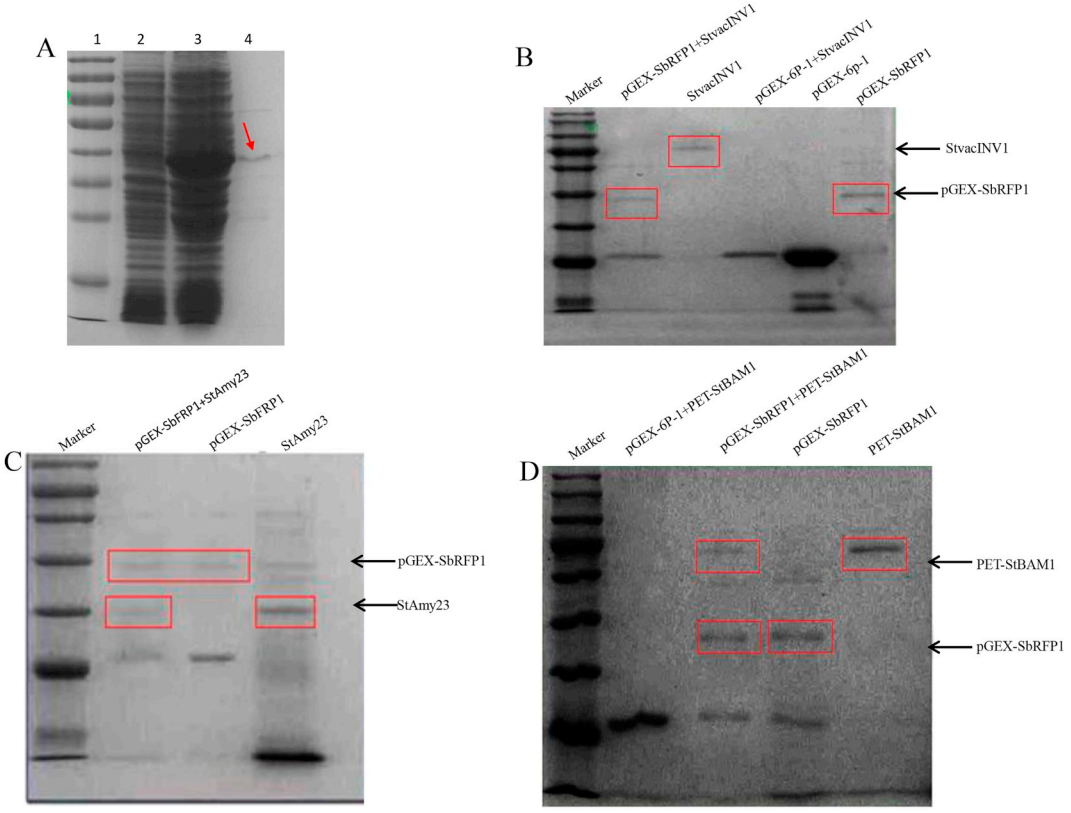

Fig. 4. Interactions for StAmy23, StBAM1, StvacINV1 and SbRFP1. A: An SDS-PAGE of pGEX-SbRFP1 protein as expression in *E. coli* cells. Lane 1, molecular marker; Lane 2, before being treated with IPTG; Lane 3, after being treated with IPTG; Lane 4, purified pGEX-SbRFP1 protein (arrow). B: Protein interaction between pGEX-SbRFP1 and StvacINV1 with GST-pull down. Lane 1, molecular marker; Lane 2, elution proteins from pGEX-SbRFP1 and StvacINV1 co-incubated; Lane 3, purified StvacINV1 protein; Lane 4, elution proteins from pGEX-6P-1 and StvacINV1 co-incubated; Lane 5, purified pGEX-6P-1 protein; Lane 6, purified pGEX-SbRFP1 protein. C: Protein interaction between pGEX-SbRFP1 and StAmy23 with GST-pull down. Lane 1, molecular marker; Lane 2, elution proteins from pGEX-SbRFP1 and StAmy23 co-incubated; Lane 3, purified pGEX-SbRFP1 protein; Lane 4, purified StAmy23 protein. D: Protein interaction between pGEX-SbRFP1 and PET-StBAM1 with GST-pull down. Lane 1, molecular marker; Lane 2, elution proteins from pGEX-6P-1 and PET-StBAM1 co-incubated; Lane 3, elution proteins from pGEX-SbRFP1 and PET-StBAM1 co-incubated; Lane 4, purified pGEX-SbRFP1 protein; Lane 5, purified PET-StBAM1 protein.

indicated that the β-amylase activity in potato tubers was decreased rapidly as the SbRFP1 concentration increased, while there was no significant change in the activity of α-amylase (Fig. 5A). In order to determine whether SbRFP1 has direct inhibitory effect on β-amylase activity, the inhibitory effect of SbRFP1 on StBAM1 was further detected. Results showed that the residual activity of StBAM1 was reduced rapidly as the SbRFP1 concentration increased to 600 ng/mL (Fig. 5B). GST protein was used as negative control in the whole experiment. All these suggested that SbRFP1 could control the accumulation of RS by interacting with β-amylase StBAM1 mainly and inhibiting its activity in cold-stored potato tubers.

To further illustrate the function of SbRFP1, we constructed a RING-motif mutant sbrfp1 by changing residues His140 and Cys150 of SbRFP1 to Try140 and Ser150. Fusion protein pGEX-sbrfp1 were purified from *E.coli* (Fig. 6A), and the inhibitory of StBAM1 by sbrfp1 was detected. With the concentration of sbrfp1 increased, the residual activity of StBAM1 did not change significantly (Fig. 6B), which indicated that sbrfp1 had no obvious inhibitory effect on StBAM1 activity. The results proved that His140 and Cys150 are important for the inhibition activity of SbRFP1 on StBAM1.

3.5. SbRFP1 possesses the activity of ubiquitin ligase E3

To evaluate whether SbRFP1 possesses E3 ubiquitin ligase activity, we tested it *in vitro* by the ubiquitination assay. The ubiquitination activity was observed in immunoblots using monoclonal antibodies of ubiquitin as a probe. The polyubiquitination of SbRFP1 was detected in the presence of E1, E2, ubiquitin and ATP as well as the positive control. However, when SbRFP1 was replaced by sbrfp1, no polyubiquitination was detected. And no clear protein polyubiquitination could be detected in the absence of any of components E1, E2, ubiquitin or ATP (Fig. 7). The result indicates that SbRFP1 possesses the E3 ubiquitin ligase activity and the conserved region of the RING finger is required for the activity. Therefore, we speculate that in potato tuber

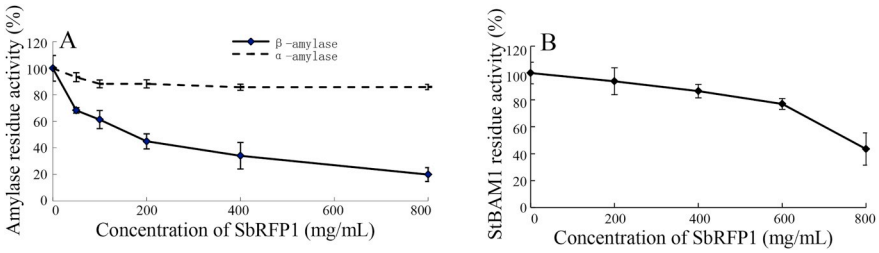

Fig. 5. The inhibitory effects of SbRFP1 protein on amylase activity. A: The inhibitory effects of SbRFP1 on α-amylase and β-amylase activity when isolated from cold-stored tubers. B: the inhibitory effects of SbRFP1 on the activity of purified StBAM1. The error bar indicates the standard error of the mean for three biological replicates.

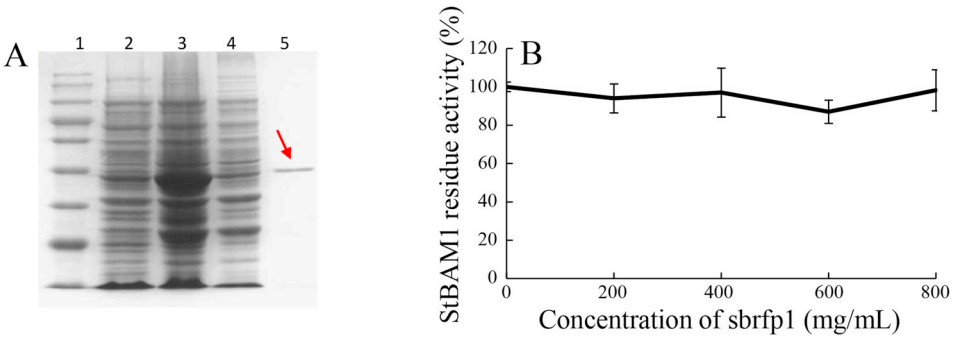

Fig. 6. The inhibitory effects of sbrfp1 protein on amylase activity. A: the purification of pGEX-sbrfp1 protein from *E. coli* cells. Lane 1, molecular marker; Lane 2, isolated total proteins before IPTG induction; Lane 3, isolated total proteins after IPTG induction; Lane 4, isolated total proteins from the soluble fraction; Lane 5, purified pGEX-sbrfp1 protein (arrow). B: the inhibitory effects of sbrfp1 on the activity of StBAM1. The error bar indicates the standard error of the mean for three biological replicates.

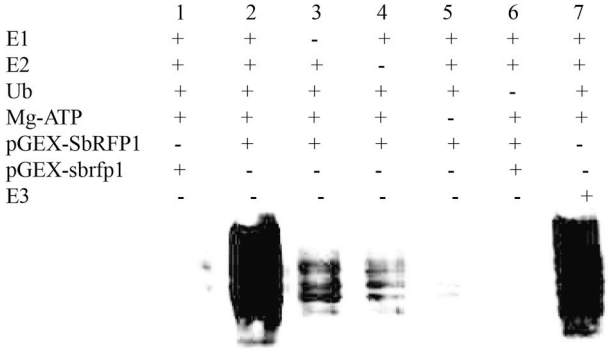

Fig. 7. SDS-PAGE of E3 ubiquitin ligase activity *in vitro*. Purified pGEX-SbRFP1 and pGEX-sbrfp1 were incubated at 37 °C for 1 h with E1, E2, ubiquitin (Ub) and ATP, respectively. Polyubiquitin chains were visualized with anti-ubiquitin antibodies. Omission of E1, E2, Ub or ATP resulted in a loss of ubiquitination. When pGEX-SbRFP1 was present instead of pGEX-sbrfp1, the polyubiquitin chains were missing.

SbRFP1 could decrease the activity of β-amylase, which may be achieved by ubiquitination and degradation of StBAM1.

4. Discussion

A major drawback of potato tubers stored at low temperature is the CIS, which affects the commercial value of the processed products. Previous research indicated that starch degradation and sucrose decomposition were considered to be the key pathways in potato CIS (Chen et al., 2012). A novel RING finger gene *SbRFP1* was cloned in our previous study, and results of transformation in potatoes confirmed its roles of slowing down starch and sucrose degradation and the accumulation of reducing sugars through inhibiting amylase and invertase activity in cold stored tubers. In this study, we found that the starch content in the OE-transgenic plant leaves of *SbRFP*1 was higher than that of the control E3 (Fig. 1), which is consistent with the starch content of *StBAM1* RI-transgenic lines, but not consistent with that of *StAmy23* or *StBAM9* RI-transgenic lines (Hou, 2013). This indicates that the effect of SbRFP1 on starch content is likely to be achieved by affecting the activity of StBAM1. Further studies by yeast two hybrid, GST-pull down and enzyme activity inhibition test confirmed that SbRFP1 could interact with StBAM1 and inhibit the activity of StBAM1, but not that of α-amylase (Figs. 4 and 5).

RING finger proteins often play important roles as ubiquitin ligase E3 through post-translational regulation of the target proteins in plants (Lee and Kim, 2011; Ning et al., 2011), and also affect the physiological processes of plants by regulating the expression of related genes (Ko et al., 2006). RING finger protein SbRFP1 which had the activity of ubiquitin ligase E3 (Fig. 7) interacted with amylase StBAM1 (Fig. 4D), and could inhibit the activity of StBAM1 directly (Fig. 5B). The results showed that SbRFP1 regulated StBAM1 at the post-translational level. And previous studies showed that over-expression of *SbRFP1* gene suppressed the expression of *StBAM1* and viceversa for the RNA interference (Zhang et al., 2013). All of these results indicate that *SbRFP1* regulates starch degradation at both transcriptional and post-translational levels. Previous studies about the effect of starch degradation on CIS mainly focused on the amylases (Solomos and Mattoo, 2005; Hou et al., 2017), but few on related regulatory genes. We previously found a regulator of the amylases named SbAI that could decrease the starch degradation and RS accumulation in cold-stored potato tubers (Zhang et al., 2014b). *SbRFP1* as another regulator of amylase can provide more powerful evidence for the effect of starch degradation on potato CIS.

Previous studies showed that RNAi silencing of *SbRFP1* resulted in a strong activation the expression of the invertase gene *StvacINV1* and the invertase activity was significantly inhibited in the OE-transgenic tubers while increased in the RI-transgenic tubers (Zhang et al., 2013). However, protein interaction analysis showed that SbRFP1 was not interacted with StvacINV1 (Fig. 4B). The results indicated that *SbRFP1* regulated *StvacINV1* only at transcriptional level without post transcriptional level. And the amylase gene *StAmy23* was induced in the *SbRFP1* RNAi silencing tubers (Zhang et al., 2013). All of these demonstrated that SbRFP1 played roles in potato CIS through transcriptional regulation of starch glycometabolism related genes and post-translational regulation of amylase protein StBAM1, which is similar with the drought tolerance related RING finger protein OsDIS1 in rice. Overexpression of *OsDIS1* reduced drought tolerance in transgenic rice plants, while RNAi silencing of *OsDIS1* enhanced drought tolerance. Microarray analysis revealed that a large number of drought-responsive genes were induced or suppressed in the *OsDIS1* overexpression plants. Yeast two-hybrid screening and coexpression assays showed that OsDIS1 interacted and degraded OsNek6, a tubulin complex-related serine/threonine protein kinase (Ning et al., 2011).

5. Conclusion

The starch content of transgenic plants confirmed that the effect of SbRFP1 on starch content is likely to be achieved by affecting the activity of StBAM1. The interacting protein analysis and ubiquitin ligase activity showed that SbRFP1 could inhibit the activity of StBAM1 by ubiquitination, thereby reducing starch degradation and reducing sugar accumulation in potato tubers. The results well elucidated the mechanism of *SbRFP1* in the process of potato CIS.

Author contributions

B. Song and C. Xie Designed the research. H. Zhang and Y. Yao performed the plant growth, leaves and tubers treatment of OE-and RNAi-SbRFP1 lines. Y. Yao and J. Hou performed the starch content and starch granule shape. Y. Yao performed subcellular localization. H. Zhang, S. Chen and Y. Yu performed vector development, protein expression and purification. H. Zhang, S. Chen, J. Hou and T. Liu performed Y2H and GST Pull-down experiment. H. Zhang and Y. Yao performed amylase activity analyses. H. Zhang and Y. Yu performed the

E3 ubiquitin ligase activity assay. H. Zhang, B. Song and C. Xie analyzed the data. H. Zhang, B. Song, J. Du and C. Xie wrote the article.

Acknowledgements

This work was supported by the grants from the National Science Foundation of China (31401437 and 31671749), the Earmarked Fund for Modern Agro-Industry Technology Research System of China (CARS-09-P07), Programs for Science and Technology Development of Henan province (172102410050), Research funding for young academic leaders of Henan University of Science and Technology (4026-13490004) and the Doctoral Foundation of Henan University of Science and Technology (4026-13480045).

References

Bhaskar, P.B., Wu, L., Busse, J.S., Whitty, B.R., Hamernik, A.J., Jansky, S.H., Buell, C.R., Bethke, P.C., Jiang, J., 2010. Suppression of the vacuolar invertase gene prevents cold-induced sweetening in potato. Plant Physiol. 154, 939–948.

Chen, M., Ni, M., 2006. Red and far-red insensitive 2, a RING-domain zinc finger protein, mediates phytochrome-controlled seedling deetiolation responses. Plant Physiol. 140, 457–465.

Chen, X., Song, B., Liu, J., Yang, J., He, T., Lin, Y., Zhang, H., Xie, C., 2012. Modulation of gene expression in cold-induced sweetening resistant potato species *Solanum berthaultii* exposed to low temperature. Mol. Genet. Genom. 287, 411–421.

Dong, C.H., Agarwal, M., Zhang, Y., Xie, Q., Zhu, J.K., 2006. The negative regulator of plant cold responses, HOS1, is a RING E3 ligase that mediates the ubiquitination and degradation of ICE1. P Natl Acad Sci USA 103, 8281–8286.

Halford, N.G., Curtis, T.Y., Muttucumaru, N., Postles, J., Elmore, J.S., Mottram, D.S., 2012. The acrylamide problem: a plant and agronomic science issue. J. Exp. Bot. 63, 2841–2851.

Han, S., Wang, Y., Zheng, X., Jia, Q., Zhao, J., Bai, F., Hong, Y., Liu, Y., 2015. Cytoplastic glyceraldehyde-3-phosphate dehydrogenases interact with ATG3 to negatively regulate autophagy and immunity in *Nicotiana benthamiana*. Plant Cell 27, 1316–1331.

Helliwell, C.A., Wesley, S.V., Wielopolska, A.J., Waterhouse, P.M., 2002. High-throughput vectors for efficient gene silencing in plants. Funct. Plant Biol. 29, 1217–1225.

Hou, J., 2013. Function Characterization and Mechanism Dissection of the Amylase Genes Related to Cold-Induced Sweetening in Potato. Dissertation, Huazhong Agricultural University, Wuhan, China.

Hou, J., Zhang, H., Liu, J., Reid, S., Liu, T., Xu, S., Tian, Z., Sonnewald, U., Song, B., Xie, C., 2017. Amylases StAmy23, StBAM1 and StBAM9 regulate cold-induced sweetening of potato tubers in distinct ways. J. Exp. Bot. 68, 2317–2331.

Jung, Y., Lee, I., Nou, I., Lee, K., Rashotte, A., Kang, K., 2013. BrRZFP1 a Brassica rapa C3HC4-type RING zinc finger protein involved in cold, salt and dehydration stress. Plant Biol. 15, 274–283.

Ko, J.H., Yang, S.H., Han, K.H., 2006. Upregulation of an Arabidopsis RING-H2 gene, *XERICO*, confers drought tolerance through increased abscisic acid biosynthesis. Plant J. 47, 343–355.

Lee, J.H., Kim, W.T., 2011. Regulation of abiotic stress signal transduction by E3 ubiquitin ligases in Arabidopsis. Mol. Cell. 31, 201–208.

Li, X.Q., Zhang, J., Luo, S., Liu, G., 2011. Effects of sampling methods on starch granule size measurement of potato tubers under a light microscope. Int. J. Plant Biol. 2, 118–122.

Lin, Y., Liu, T., Liu, J., Liu, X., Ou, Y., Zhang, H., Li, M., Sonnewald, U., Song, B., Xie, C., 2015. Subtle regulation of potato acid invertase activity by a protein complex of invertase, invertase inhibitor, and Sucrose Nonfermenting1-Related Protein Kinase. Plant Physiol. 168, 1807–1819.

Liu, X., Song, B., Zhang, H., Li, X.-Q., Xie, C., Liu, J., 2010. Cloning and molecular characterization of putative invertase inhibitor genes and their possible contributions to cold-induced sweetening of potato tubers. Mol. Genet. Genom. 284, 147–159.

Mottram, D.S., Wedzicha, B.L., Dodson, A.T., 2002. Food chemistry: acrylamide is formed in the Maillard reaction. Nature 419, 448–449.

Nielsen, T.H., Deiting, U., Stitt, M., 1997. A [beta]-amylase in potato tubers is induced by storage at low temperature. Plant Physiol. 113, 503–510.

Ning, Y., Jantasuriyarat, C., Zhao, Q., Zhang, H., Chen, S., Liu, J., Liu, L., Tang, S., Park, C.H., Wang, X., Liu, X., Dai, L., Xie, Q., Wang, G.L., 2011. The SINA E3 ligase OsDIS1 negatively regulates drought response in rice. Plant Physiol. 157, 242–255.

Preiss, J., 1982. Regulation of the biosynthesis and degradation of starch. Annu. Rev. Plant Physiol. 33, 431–454.

Shepherd, L.V.T., Bradshaw, J.E., Dale, M.F.B., McNicol, J.W., Pont, S.D.A., Mottram, D.S., Davies, H.V., 2010. Variation in acrylamide producing potential in potato: segregation of the trait in a breeding population. Food Chem. 123, 568–573.

Solomos, T., Mattoo, A.K., 2005. Starch-sugar metabolism in potato (*Solanum tuberosum* L.) tubers in response to temperature variations. Gene. Improv. Solanaceous Crops 1, 209–234.

Tai, H.C., Besche, H., Goldberg, A.L., Schuman, E.M., 2010. Characterization of the brain 26S proteasome and its interacting proteins. Front. Mol. Neurosci. 3, 1–12.

Xin, Z., Browse, J., 2000. Cold comfort farm: the acclimation of plants to freezing temperatures. Plant Cell Environ. 23, 893–902.

Zhang, H., Hou, J., Liu, J., Xie, C., Song, B., 2014a. Amylase analysis in potato starch degradation during cold storage and sprouting. Potato Res. 57, 47–58.

Zhang, H., Liu, J., Hou, J., Yao, Y., Lin, Y., Ou, Y., Song, B., Xie, C., 2014b. The potato amylase inhibitor gene *SbAI* regulates cold-induced sweetening in potato tubers by modulating amylase activity. Plant Biotechnol. J 12, 984–993.

Zhang, H., Liu, X., Liu, J., Ou, Y., Lin, Y., Li, M., Song, B., Xie, C., 2013. A novel RING finger gene, *SbRFP1*, increases resistance to cold-induced sweetening of potato tubers. FEBS Lett. 587, 749–755.

Zhang, X., Garreton, V., Chua, N.H., 2005. The AIP2 E3 ligase acts as a novel negative regulator of ABA signaling by promoting ABI3 degradation. Genes Dev. 19, 1532–1543.